The EMBO Journal (2010) 29, 727–739 | © 2010 European Molecular Biology Organization | All Rights Reserved 0261-4189/10
www.embojournal.org

THE EMBO JOURNAL

SLR-2 and JMJC-1 regulate an evolutionarily conserved stress-response network

Natalia V Kirienko and David S Fay*

Department of Molecular Biology, College of Agriculture, University of Wyoming, Laramie, WY, USA

Maintaining a homeostatic interaction with the environment is crucial for the growth, survival, and propagation of all living organisms. Reestablishment of equilibrium after stress is achieved by the activation of complex transcriptional-response networks, many of which remain poorly understood. Here, we report that the zinc-finger protein, SLR-2, is a master stress regulator and is required for the normal response to pleiotropic stress conditions in *Caenorhabditis elegans*. Using bioinformatical tools, we identified an evolutionarily conserved nucleotide motif present in *slr-2* stress-responsive genes and show that this motif is sufficient for stress induction under a variety of conditions. We also demonstrate that JMJC-1, a conserved Jumonji C domain protein, acts downstream of SLR-2 to mediate stress response in *C. elegans*. Moreover, the role of JMJC-1 in stress response is conserved in *Drosophila* and mammals. Finally, we provide evidence that the SLR-2–JMJC-1 pathway functions independently of the well-studied DAF-16/FOXO1 network. These findings point to a previously unrecognized phylogenetically conserved master stress-response pathway in metazoa.

The EMBO Journal (2010) **29,** 727–739. doi:10.1038/emboj.2009.387; Published online 7 January 2010
Subject Categories: signal transduction; chromatin & transcription
Keywords: *C. elegans*; *jmjc-1*; microarray; *slr-2*; stress

Introduction

All living organisms maintain a homeostatic interaction with their environment that is essential for growth, survival, and reproduction (Johnson *et al*, 2000, 2002; Mukhopadhyay and Tissenbaum, 2007). Unfavourable conditions, such as hypoxia, oxidative stress, hyperthermia, hypertonicity, infection with a pathogen, or redox stress, destabilize this interaction. When this occurs, a range of cellular strategies is used to regain homeostasis. One of the most important methods for this reacquisition is the activation of transcriptional regulators that direct the expression of genes that initiate repair mechanisms to counter imbalances and promote survival. Typically, a specific environmental perturbation leads to a characteristic transcriptional-response pattern, often controlled by one or more transcription factors (Henderson and Johnson, 2001; An and Blackwell, 2003; Baumeister *et al*, 2006; Berdichevsky *et al*, 2006; Kell *et al*, 2007; Panowski *et al*, 2007). Notably, many stress-response networks are exceptionally well conserved, and our understanding of stress regulation in humans has been greatly aided by the study of model systems (Hertweck *et al*, 2003; Berdichevsky and Guarente, 2006).

With its many experimental attributes, *Caenorhabditis elegans* has emerged as an excellent system for the study of stress networks and the underlying principles that govern their regulation. One recurring theme is that the majority of stress-response pathways exhibit some degree of pleiotropy in their activating conditions. For example, HSF-1/HSF1 is activated in response to hyperthermia, protein misfolding, and bacterial infection (Garigan *et al*, 2002; Singh and Aballay, 2006). SKN-1, the *C. elegans* ortholog of the human NRF2 protein, in conjunction with the kinases PDHK-2/PDK3 and NEKL-2/NEK8, is activated by oxidative stress (Kell *et al*, 2007). SKN-1 is also known to be activated by heat and sodium azide (An and Blackwell, 2003). Perhaps the most versatile stress-responsive transcription factor described in *C. elegans* is DAF-16/FOXO1. For example, *daf-16* has been shown to be necessary for expression of heat shock response genes (Hsu *et al*, 2003) and functional DAF-16::GFP fusion proteins translocate from the cytoplasm to the nucleus on heat stress (Henderson and Johnson, 2001; Lin *et al*, 2001; Hsu *et al*, 2003; Oh *et al*, 2005). In addition, overexpression of DAF-16 confers greater resistance to heat and UV radiation (Murakami and Johnson, 1996; Henderson and Johnson, 2001) as well as osmotolerance (Lamitina and Strange, 2005). Furthermore, *daf-16* activity is necessary for the UV resistance characteristic of insulin pathway signalling mutants in *C. elegans*, such as *daf-2* and *age-1* (Murakami and Johnson, 1996), the oxidative (Honda and Honda, 1999) and hypertonic (Lamitina and Strange, 2005) stress resistance observed in *daf-2* mutants, and heavy metal stress resistance in *age-1* mutants (Barsyte *et al*, 2001).

A number of stress-response factors in *C. elegans* also show partial genetic redundancy, indicating some degree of functional overlap. For example, PHA-4/FOXA, SKN-1, and DAF-16 all show some level of involvement in the oxidative-stress response (Honda and Honda, 1999; Kell *et al*, 2007; Panowski *et al*, 2007). In addition, HSF-1 shows partial redundancy with DAF-16 in the heat shock response (Hsu *et al*, 2003). Nonetheless, the ubiquity of DAF-16 in pleiotropic stress responses is unique, thereby classifying DAF-16 as a master controller of the stress response in *C. elegans*.

Previously, we have reported a role for SLR-2, a Zn-finger protein, in the maintenance of intestinal functions and gene regulation in *C. elegans* (Kirienko *et al*, 2008). Here, we provide evidence that SLR-2 and an additional transcriptional regulator, JMJC-1, have a function in the generalized stress

*Corresponding author. Department of Molecular Biology, College of Agriculture, University of Wyoming, Dept 3944, 1000 E. University Avenue, Laramie, WY 82071, USA. Tel.: +1 307 766 4961; Fax: +1 307 766 5098; E-mail: davidfay@uwyo.edu

Received: 18 May 2009; accepted: 1 December 2009; published online: 7 January 2010

response in *C. elegans*. Our studies indicate that SLR-2 and JMJC-1 control the regulation of hundreds of stress-associated target genes through an evolutionarily conserved nucleotide motif. Notably, we provide experimental evidence that this master stress-response network is phylogenetically conserved in both *Drosophila* and mammals.

Results

An evolutionarily conserved stress motif is strongly enriched in slr-2-responsive genes

We have reported earlier on the role of the *C. elegans* Zn-finger protein SLR-2 in larval nutrient usage (Kirienko *et al*, 2008). To gain further insight into the functions of SLR-2, we used computational methods to group genome-wide microarray data obtained from both N2 (Kirienko and Fay, 2007) and *slr-2* mutant larvae (Kirienko *et al*, 2008) into 45 expression clusters (Supplementary Figure S1). We next analysed the upstream non-coding regions of genes from each cluster to identify overrepresented nucleotide sequences (Kirienko and Fay, 2007). This search showed a single motif, TCTGCGTCTCT (Figure 1A and B), that was enriched by up to 30% in clusters with downregulated genes (e.g. Clusters 14 and 45; Supplementary Figure S1). Conversely, clusters with genes expressed at higher levels in *slr-2* mutants, as compared with wild type, showed no enrichment of this motif (e.g. Cluster 16; Supplementary Figure S1). Microarray findings for genes containing the motif were further corroborated by quantitative real-time reverse transcription–PCR (qRT–PCR) (Figure 2A and B; data not shown).

The identified motif has several noteworthy characteristics: (1) 90% of genes that contain the motif were downregulated in *slr-2* mutants. (2) The motif was enriched in *slr-2*-responsive genes as compared with the genome-wide average ($P<0.001$). (3) The motif showed a bias towards transcriptional start sites and (4) was found multiple times within a number of genes (Figure 1C). Additionally, a data set of 223 motif-containing genes showed greater connectivity by network analysis (Lee *et al*, 2008) than did multiple identically sized sets of randomly selected genes (177 connections versus an average of 27.4 for random gene sets; $P<0.001$; Supplementary Figure S2).

To determine whether this motif is evolutionarily conserved, we examined the upstream regions of putative orthologs of motif-containing genes in other species. *C. briggsae*, a sister nematode species, showed ~60% motif retention among orthologous genes (data not shown). In a similar search of putative orthologs in *Drosophila melanogaster*, we observed that the element is highly enriched when compared with the genome average; the motif was present in 24% of orthologs with upstream sequences, which is ~3.4 times higher than in 100 identically sized random gene sets (Supplementary Figure S3; $P<0.001$). Similar searches in both mice and humans showed that the motif was present in these organisms as well. In humans, 42% of putative orthologs (with available upstream sequence) retained the motif, which is 2.5 times higher than its occurrence among 100 random gene sets (Supplementary Figure S3; $P<0.001$). Thus, our computational analysis implicated a network of orthologous genes that contain a phylogenetically conserved promoter motif.

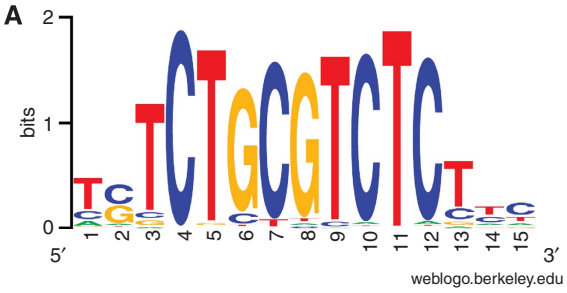

B

#	Gene	Fold	Motif
1	*aat-4*	–1.8	5′-TCTCTGCTTCTCT-3′
2	C34C12.8	–2.6	5′-TGTCTGCGTCTCC-3′
3	C39E9.8	–1.5	5′-TGTCTGCGTCTTG-3′
4	*crh-1*	–2.0	5′-TGTCTGCGTCTCT-3′
5	*cyp-33*	–2.0	5′-TACCTGCGTCTCC-3′
6	*dnj-7*	–2.2	5′-TGTCTGCGTCTAC-3′
7	F15D3.6	–2.9	5′-TGTCTGCGTCTCT-3′
8	F32D8.3	–2.2	5′-CGTCTGCGTCTCT-3′
9	F56H1.5	–1.8	5′-TGTCTGCGTCTCT-3′
10	H25P06.1	–2.3	5′-CGCCTGCGTCTCT-3′
11	*hif-1*	–1.8	5′-TCTCTGCGTCTCC-3′
12	*hsp-3*	–1.5	5′-ACTCTGCGTCTCT-3′
13	*lin-40*	–1.6	5′-TTTCTGCGTCTCT-3′
14	*rbc-1*	–2.0	5′-CGTCTGCGTCTCT-3′
15	*toh-1*	–1.9	5′-TCTCTGCGTCTCC-3′
16	*ubc-3*	–2.2	5′-TGTCTGCGTCTCT-3′
17	*ugt-28*	–2.1	5′-CTTCTGCGTCTCA-3′

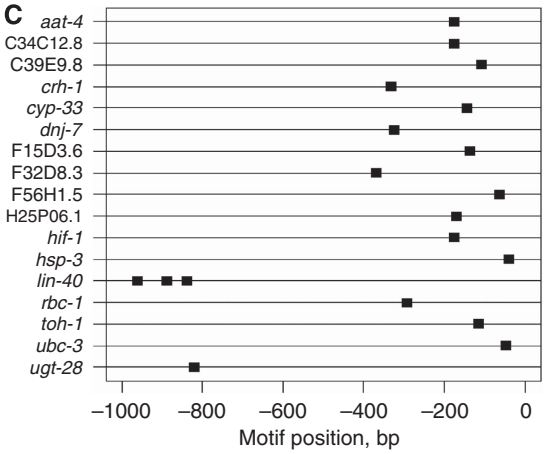

Figure 1 Identification of a *slr-2*-responsive motif. (**A**) Logogram of a 11-nucleotide motif identified by K-means clustering and MEME that was strongly enriched in multiple clusters of *slr-2*-responsive genes. (**B**) Seventeen examples of high-scoring genes that contain the consensus site along with their fold changes in *slr-2* mutants. (**C**) Location of the motif within promoter regions shows a bias towards transcriptional start sites, and the motif is found in multiple copies in some genes.

A literature search showed that this motif had been identified earlier in several independent studies in *C. elegans*. Original reports identified a mismatched portion of the motif (GGGTGTC; the common portion is underlined) in a heat shock-associated site (GuhaThakurta *et al*, 2002) and noted the presence of the motif within inverted repeats in the regulatory regions of *hsp-16.2*, *hsp-16.48*, *hsp-16.1*, and *hsp-16.41* (Candido *et al*, 1989). Later reports showed this motif (termed ESRE, for ethanol and stress-response element)

A

	Gene		Gene
1	*aat-4*	10	H25P06.1
2	C34C12.8	11	*hif-1*
3	C39E9.8	12	*hsp-3*
4	*crh-1*	13	*lin-40*
5	*cyp-33*	14	*rbc-1*
6	*dnj-7*	15	*toh-1*
7	F15D3.6	16	*ubc-3*
8	F32D8.3	17	*ugt-28*
9	F56H1.5		

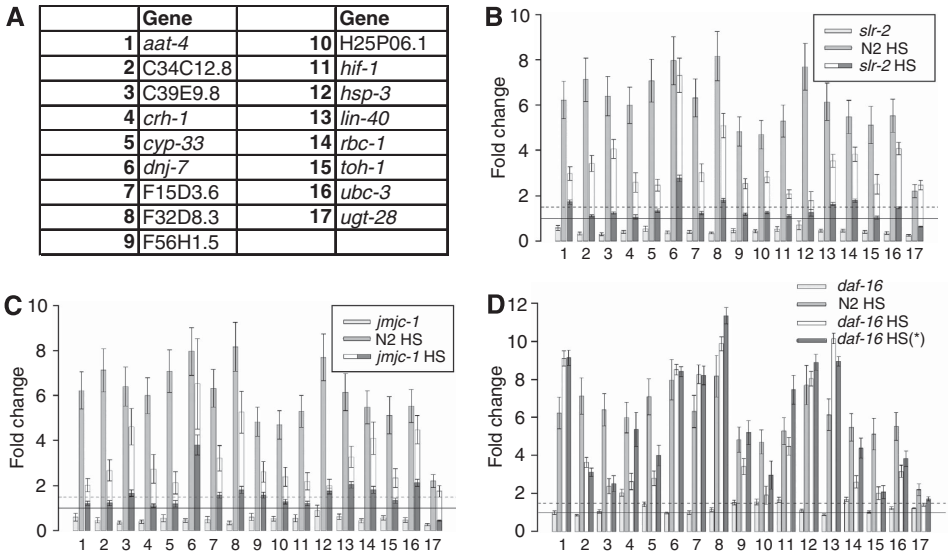

Figure 2 Heat shock induction of ESRE genes is attenuated in *slr-2* and *jmjc-1* mutants. (**A**) 17 genes selected for qRT–PCR analysis in *slr-2*(*ku297*) and *jmjc-1*(*tm3525*) mutants on the basis of expression level and match to ESRE consensus motif. (**B**) After a 12 h exposure to a 30°C, non-lethal heat shock, ESRE target genes showed an upregulation in N2 and a reduction in the levels of induction in *slr-2*(*ku297*) mutants. Light grey bars represent expression of genes in unstressed *slr-2*(*ku297*) mutants normalized to unstressed wild-type (N2) controls, grey bars represent expression of genes in heat-shocked wild-type (N2) worms normalized to unstressed, wild-type controls, and mixed bars represent gene expression in heat-shocked *slr-2*(*ku297*) mutants normalized to either unstressed wild-type (N2) controls (dark portion) or unstressed *slr-2*(*ku297*) mutants (light portion). (**C**) After a 12 h exposure to a 30°C non-lethal heat shock, ESRE target genes showed a attenuation of upregulation in *jmjc-1*(*tm3525*) mutants. Light grey bars represent expression of genes in *jmjc-1*(*tm3525*) mutants normalized to unstressed wild-type (N2) controls, grey bars represent expression of genes in heat-shocked wild-type (N2) worms normalized to unstressed, wild-type controls, and mixed bars represent gene expression in heat-shocked *jmjc-1*(*tm3525*) mutants normalized to either unstressed wild-type controls (dark portion) or unstressed *jmjc-1*(*tm3525*) mutants (light portion). (**D**) After a 12 h exposure to a 30°C non-lethal heat shock, most ESRE target genes showed upregulaltion in *daf-16(mu86)* mutants. Light grey bars represent expression of genes *daf-16(mu86)* normalized to unstressed wild-type (N2) controls, grey bars represent expression of genes in heat-shocked wild-type (N2) worms normalized to unstressed, wild-type controls, the white bars represent gene expression in heat-shocked *daf-16(mu86)* mutants normalized to unstressed *daf-16(mu86)*, and dark grey bars represent gene expression in heat-shocked *daf-16(mu86)* mutants normalized to unstressed wild-type. In (**B**–**D**), data are the means of three biological replicates in which each replicate measured in triplicate; error bars represent s.e.m. and solid and dashed lines represent 1- and 1.5-fold change, respectively. Additional statistical information for (**B**–**D**) is available in Supplementary Table S1A–C.

to be necessary for the induction of genes after ethanol and hypoxic stress and heat shock (Hong *et al*, 2004; Kwon *et al*, 2004). From its identification in these diverse conditions as well as our bioinformatical analysis, we hypothesized that the ESRE motif may function as an evolutionarily conserved master stress control element.

To test this hypothesis computationally, microarray data were obtained from *C. elegans* GEO data sets for multiple stress conditions, including oxidative stress (GSE9301), redox stress (Falk *et al*, 2008), and *Pseudomonas* infection (Troemel *et al*, 2006). As DAF-16 activity has proven to be central to many aspects of stress resistance (Henderson and Johnson, 2001; Oh *et al*, 2006), microarray data were also obtained for *daf-16* mutants (Murphy *et al*, 2003; McElwee *et al*, 2004). Differentially expressed genes were either identified *de novo* from the GeneChip data sets as described earlier (Kirienko and Fay, 2007) or were taken from the authors' lists in the case of spotted arrays (GuhaThakurta *et al*, 2002; Kwon *et al*, 2004). The upstream promoter regions of differentially expressed genes were then searched for the presence of the ESRE motif.

When combined, the microarray data sets included 540 differentially expressed genes that contain the ESRE motif, with 114 occurring in more than one data set. The top 35 genes, as determined by differential expression under multiple stress conditions, were then used to derive an unbiased ESRE position weight matrix (PWM; Supplementary Figure S4). Network analysis was used to verify that the number of connections among genes with the refined motif was greater than that in identically sized random gene sets. Moreover, because these genes were, *prima facie*, coexpressed, we removed this criterion from the list when determining the number of interactions, leaving such categories as genetic interactions, protein–protein interactions, and interactions in other species. Again, ESRE-containing genes showed a much higher level of interconnectivity than in 500 identically sized random gene sets (35 edges in the core network as compared with an average of 7 in random sets, $P<0.001$; data not shown). These combined bioinformatic and transcriptome data indicate the existence of an evolutionarily conserved stress network and further suggest that network regulation may occur through the ESRE motif.

The ESRE motif promotes stress-induced gene activation in a SLR-2-dependent manner

Previous studies indicated that the ESRE motif was required for the robust induction of several genes in response to stress (Hong *et al*, 2004; Kwon *et al*, 2004). To determine whether or not the ESRE motif is sufficient to drive expression after stress, we generated a reporter construct containing three tandem ESRE motifs (3X-ESRE) upstream of a promoterless GFP (Figure 3A). This construct, in conjunction with a vector control that did not contain the 3X-ESRE, was used to generate strains carrying *rol-6(gf)*-marked extra-chromosomal arrays. We observed robust GFP induction after a 30°C heat shock in 9/9 independent 3X-ESRE strains analysed,

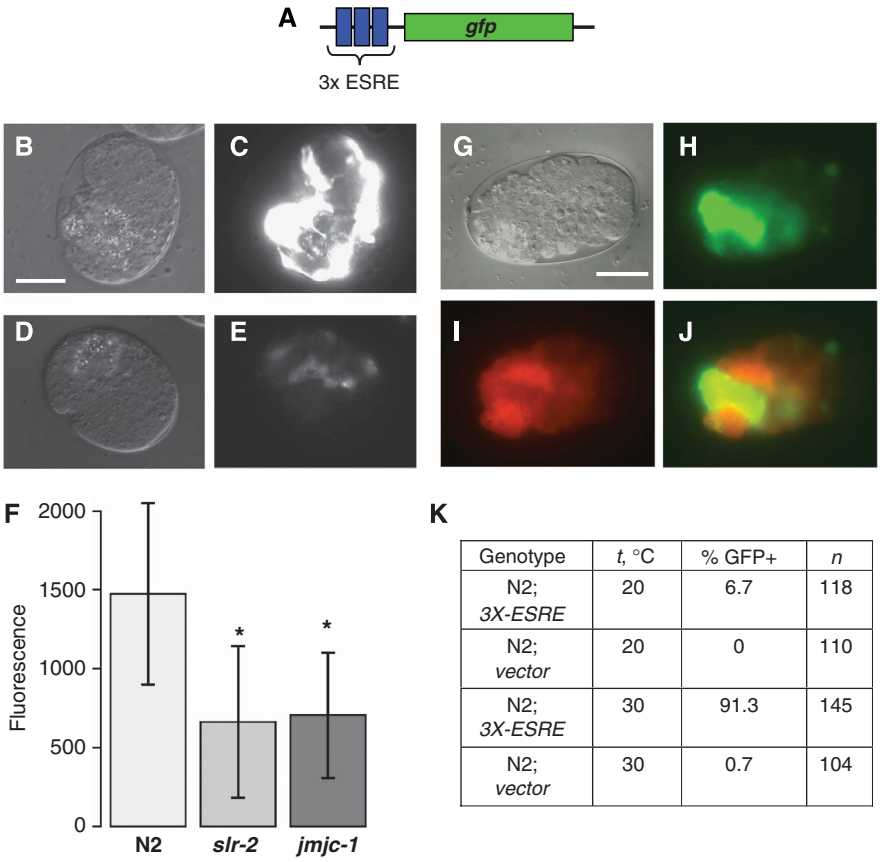

K

Genotype	*t*, °C	% GFP+	*n*
N2; *3X-ESRE*	20	6.7	118
N2; *vector*	20	0	110
N2; *3X-ESRE*	30	91.3	145
N2; *vector*	30	0.7	104

Figure 3 The ESRE motif confers SLR-2–JMJC-1-dependent stress-induced activation. (**A**) A cartoon representation of the 3X-ESRE::GFP construct. (**B–C**) DIC (**B**) and GFP (**C**) photomicrograph of a wild-type (N2) embryo containing 3X-ESRE::GFP along with the *rol-6(gf)* marker that has been subjected to a 30°C heat shock. (**D–E**) DIC (**D**) and GFP (**E**) photomicrograph of *slr-2*(*ku297*) mutant embryo carrying the same array as depicted in (**B–C**) subjected to a 30°C heat shock. (**F**) Background-normalized quantification of fluorescence in heat-shocked, wild-type, *slr-2*(*ku297*), and *jmjc-1*(*tm3525*) embryos carrying an identical 3X-ESRE [*rol-6(gf)*] array subjected to a 30°C heat shock. (**G–J**) DIC (**G**), GFP (**H**), RFP (**I**), and GFP/RFP-merged (**J**) photomicrographs of a wild-type (N2) embryo carrying 3X-ESRE::GFP and the *sur-5*::RFP marker that has been subjected to a 30°C heat-shock. (**K**) Table showing relative frequencies of GFP expression in lines with 3X-ESRE::GFP, or a control without the 3X-ESRE, at 20 or 30°C. In (**F**), all images were taken using the same gain and exposure time; asterisks indicate statistical significance, $P < 0.01$, $n = 40–50$. Error bars in (**F**) represent standard deviation (s.d.). Scale bar: 10 μm in panels (**B–E**) and (**G–J**).

whereas 0/4 control strains exhibited GFP expression (Figure 3B–E; Supplementary Figure S6F–G; and data not shown). Similar results were also observed for ethanol, oxidative, and hypertonic stress (data not shown).

To test directly for the efficiency of induction by 3X-ESRE, we also generated strains carrying a *sur-5*::RFP co-injection marker that is strongly expressed throughout development. Consistent with the above findings, stress-induced GFP activation was observed in 3/3 3X-ESRE lines and 0/3 vector control lines. Moreover, stress-induced GFP expression was observed in >90% of embryos that carried the 3X-ESRE array versus 1% for embryos containing control arrays (Figure 3G–K; Supplementary Figure S6B–E). Finally, stress-induced expression was also observed using a construct that placed the 3X-ESRE in *cis* to a Δ*pes-10* minimal promoter driving GFP (Gaudet *et al*, 2004; Supplementary Figure S6I–L; and data not shown). We note that the tissue-specific expression pattern of the 3X-ESRE::GFP construct differed between strains carrying the *rol-6(gf)* and *sur-5*::RFP markers, suggesting some additional influence of *cis*-regulatory elements present on the arrays (also see Discussion).

Expression of 3X-ESRE::GFP in stressed animals (containing either *rol-6(gf)* or *sur-5*::RFP-marked arrays) was largely confined to embryos and L1 larvae, indicating that the ESRE motif is sufficient for the activation of gene expression specifically during early development. Previous studies, as well as our present findings, however, also indicate a clear requirement for the ESRE motif in stress-dependent activation at later stages. Furthermore, young embryos placed directly onto stress plates also exhibited strong upregulation of the 3X-ESRE reporter indicating that maternal input is not required for ESRE induction. In addition, stress induction specifically in parental animals (but not embryos) was not sufficient to activate 3X-ESRE::GFP expression in F1 progeny, further indicating that ESRE induction in embryos is autonomous. Finally, consistent with the observed role for SLR-2 in the regulation of many endogenous ESRE genes, stress-induced activation of the 3X-ESRE reporter was attenuated in *slr-2* mutants (Figure 3D–F). This latter result indicates that SLR-2 is required for the robust induction of ESRE genes after stress as well as the maintenance of basal expression levels of ESRE genes in non-stressed animals.

To determine the induction pattern of ESRE-containing genes, we examined expression levels of a panel of 17 genes with this motif after heat shock in wild-type animals (Figure 2A and B). ESRE genes exhibited moderate upregulation

by 4 h; by 12 h, all but one of the genes increased expression levels by ~five- to eight-fold (Figure 3A and B; Supplementary Figure S6A–C). In contrast, upregulation of ESRE-containing genes was strongly attenuated in *slr-2* mutants (Figure 3B; Supplementary Figure S6A–C), showing a requirement for SLR-2 in the activation of endogenous ESRE genes after stress. This reduction in upregulation was most dramatic when gene expression in *slr-2* mutants was normalized to N2 background levels (Figure 2B, dark grey bars; see legend for details). We also note some variability in the level of differential expression among the genes tested. For example, *dnj-7* did not show attenuation of upregulation in *slr-2* mutants, possibly because *dnj-7* is also regulated by DAF-16 (McElwee *et al*, 2003), which may in some cases act redundantly with SLR-2 to control aspects of the stress response (also see below).

To further corroborate the role of ESRE genes in the stress response, we assayed expression of several well-established GFP stress reporters in wild type and *slr-2* mutants. These reporters included *hsp-16.2* (Link *et al*, 1999; Sampayo *et al*, 2003; Wu *et al*, 2006) and *aip-1* (Hassan *et al*, 2009) for heat shock, *gpdh-1* (Lamitina *et al*, 2006) for hyperosmotic stress, and *gst-4* (Link and Johnson, 2002; Leiers *et al*, 2003; Hasegawa *et al*, 2007) for oxidative stress. Notably, *slr-2* mutants showed markedly attenuated responses with three of the four reporters: *hsp-16.2*, *gpdh-1*, and *aip-1* (Supplementary Figure S7). This correlates with the presence of an ESRE motif in the promoter regions of these genes. In contrast, *gst-4* does not contain a recognizable ESRE motif and did not show attenuation of expression in *slr-2* mutants after oxidative stress (Supplementary Figure S7), a finding confirmed by quantification of GFP (see legend for Supplementary Figure S7). Moreover, *gst-4* is directly induced by SKN-1 under conditions of oxidative stress (Kell *et al*, 2007; Kahn *et al*, 2008).

SLR-2 functions in the response to pleiotropic stress

As *slr-2*-responsive ESRE genes were upregulated under a variety of stress conditions, we examined *slr-2* expression after stress treatment. We began by quantifying the expression of a *slr-2* transcriptional reporter ($P_{slr\text{-}2}$::GFP) in response to heat shock. Although the immediate response was minimal, showing ~1.2-fold higher expression after 1 h, expression increased to 4.5-fold by 12 h (Figure 4A). Similar levels of upregulation after heat shock were observed for both the transcriptional reporter and endogenous *slr-2* mRNA, as determined by qRT–PCR (Figure 4B). Decay of the $P_{slr\text{-}2}$::GFP reporter, after a return to standard temperatures, was gradual, mirroring the pattern of *slr-2* upregulation (data not shown). We also examined *slr-2* levels after exposure to hypertonic, ethanol, and oxidative stress. Under all conditions, we observed a similar timing and magnitude of *slr-2* upregulation (Figure 4C), suggesting a general role for *slr-2* in the adaptation to stress.

Given that (1) the basal levels of hundreds of ESRE genes were downregulated ~two-fold in *slr-2* mutants as compared with wild type and (2) the induction of ESRE genes after stress is strongly attenuated in *slr-2* mutants, we hypothesized that *slr-2* mutants may be hypersensitive to stress. To test this, we assayed four stress conditions: heat shock and oxidative, ethanol, and hypertonic stresses. In the case of heat and oxidative stress, *slr-2* mutants exhibited significantly

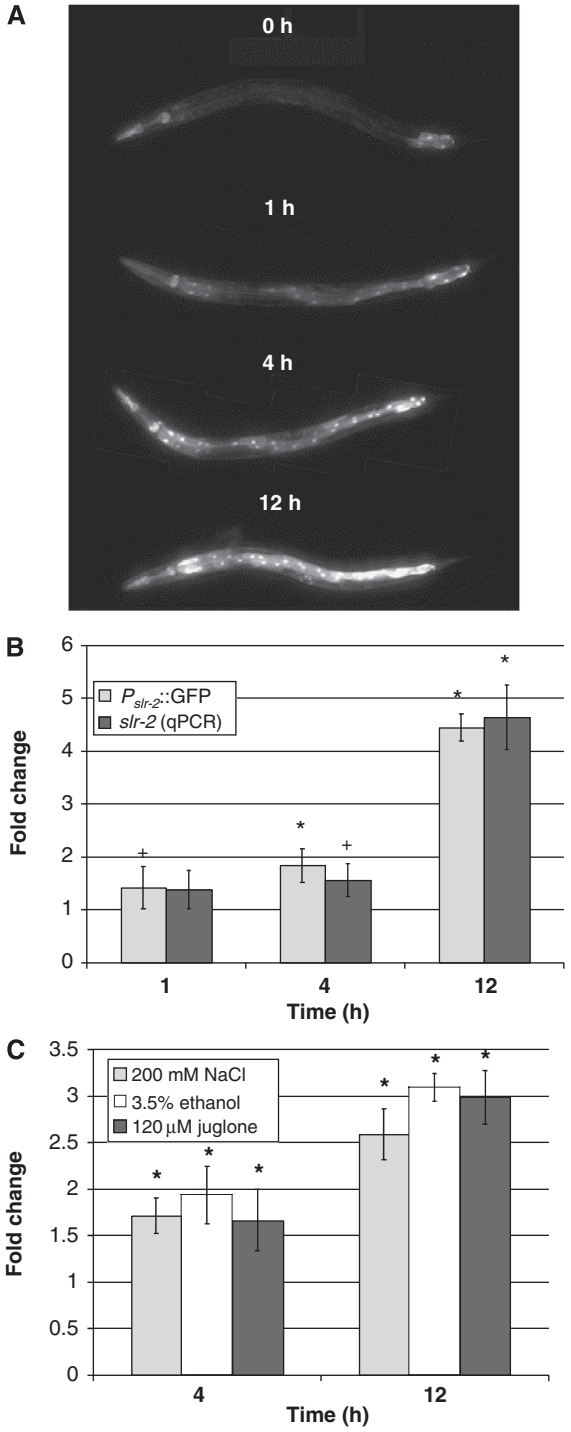

Figure 4 *slr-2* is responsive to heat shock in a time-dependent manner. (**A**) GFP fluorescence of a $P_{slr\text{-}2}$::GFP transcriptional fusion reporter expression in response to a 30°C non-lethal heat shock over a 12 h period. Enhanced expression was observed by 1 h and increased steadily for at least 12 h. (**B**) Both *slr-2* mRNA transcription (black, measured by qRT–PCR) and a $P_{slr\text{-}2}$::GFP transcriptional fusion reporter (grey, measured by fluorescence) displayed nearly identical, time-dependent increases in response to 30°C heat-shock over a 12 h period. Unstressed *slr-2* controls were used for normalization for qRT—PCR. (**C**) Quantification of $P_{slr\text{-}2}$::GFP fluorescence intensities at 4 and 12 h after exposure to non-lethal hypertonic, ethanol, and oxidative stresses. In (**B**) and (**C**), asterisks indicate $P<0.01$. In (**B**), plus sign indicates $P<0.05$. Error bars in (**B**) and (**C**) represent standard error of the mean (s.e.m.). In (**B**) and (**C**), all images were taken using the same gain and exposure time ($n\sim50$).

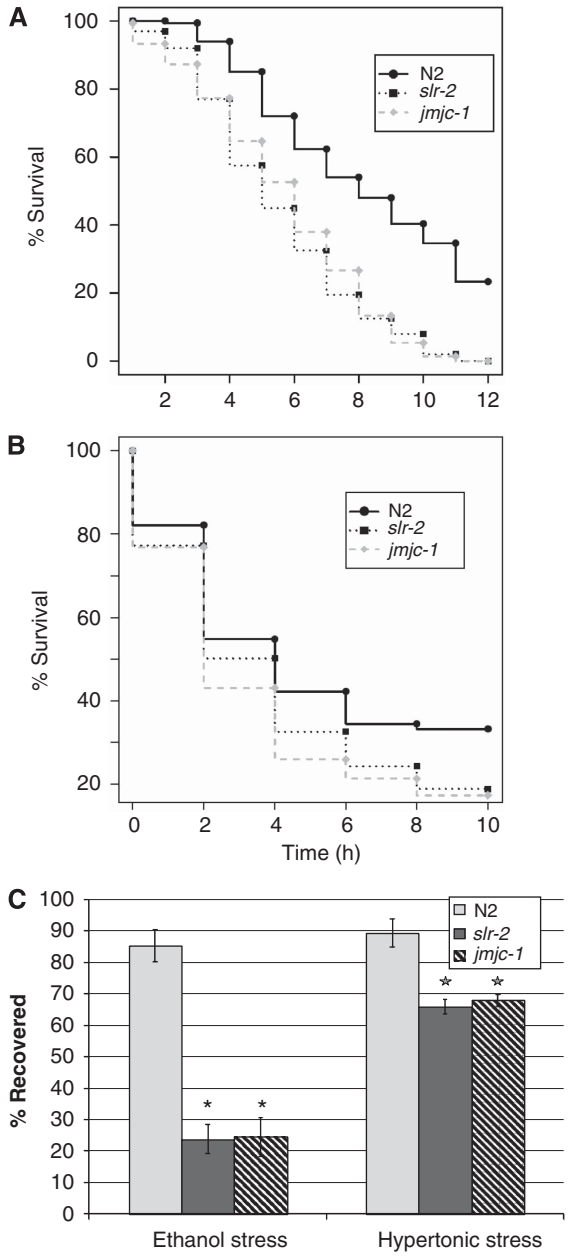

Figure 5 SLR-2 and JMJC-1 are integral to survival under stress conditions. (**A**) After exposure to a 12 h lethal heat shock (37°C), both *slr-2*(*ku297*) and *jmjc-1*(*tm3525*) mutants showed reduced survival relative to wild type (N2; $P<0.001$, $n=300$). (**B**) *slr*-2 and *jmjc-1* mutants displayed diminished survival under conditions of severe oxidative stress (160 μM juglone; $P<0.001$, $n=250$). (**C**) When exposed to brief (30 min), acute ethanol, or hypertonic stresses, *slr-2* and *jmjc-1* mutants showed reduced recovery after 30 min (asterisks, $P<0.001$, $n=200$).

decreased survival relative to wild type (Figure 5A and B; $P<0.001$). In addition, as compared with wild type, a smaller proportion of *slr-2* mutants exhibited recovery within 30 min after exposure to acute ethanol and salt stress (Figure 5C $P<0.001$). These functional assays confirm that SLR-2 has an important function in the response to pleiotropic stresses. We note that the impact of *slr-2* loss-of-function on different stresses is variable and may be at least partially attributable to the presence of redundant stress response systems (e.g. SKN-1 may independently mediate the response to oxidative stress; Kell *et al*, 2007; Kahn *et al*, 2008). Furthermore, the heightened sensitivity of *slr-2* mutants at early time points is consistent with the reduced basal levels of ESRE gene expression in this background.

The SLR-2–ESRE network functions independently of the DAF-16/FOXO pathway

DAF-16 is a central regulator of pleiotropic stress responses in *C. elegans* (Henderson and Johnson, 2001; McElwee *et al*, 2003; Oh *et al*, 2006). Several bioinformatical lines of evidence do, however, indicate that the ESRE stress network is DAF-16 independent. First, genes that contain a DAF-16 motif, as identified in a microarray study (McElwee *et al*, 2004), were not overrepresented among *slr-2*-responsive genes (data not shown). Moreover, genes that possess an ESRE motif were not overrepresented in *daf-16* microarray studies (Murphy *et al*, 2003; McElwee *et al*, 2004); 7 and 8.6% of *daf-16*-target genes contained an ESRE motif as compared with 9% of genes in the whole genome. In addition, there is only a 1% overlap in genes that are upregulated in both *slr-2* and *daf-16* mutants (Class II genes, as defined in Murphy *et al*, 2003). We note that a higher correlation (~30%) is observed between genes that are downregulated in both *slr-2* and *daf-16* mutants (Class I genes); the majority of genes in this overlap, however, posses an ESRE motif and may therefore be regulated independently by both DAF-16 and SLR-2. Finally, we measured the frequency of DAF-16-binding sites (TTRTTTAC) (Furuyama *et al*, 2000) in ESRE genes, and in 50 identically sized random gene sets, we observed that DAF-16 sites were, if anything, slightly underrepresented in ESRE genes; 22% of ESRE genes contained a putative DAF-16-binding site as compared with 30% in random data sets ($P<0.05$).

To verify experimentally that DAF-16 is not involved in the regulation of ESRE genes, we used qRT–PCR to determine expression of the ESRE gene panel in both a DAF-16-overexpressing strain (Henderson and Johnson, 2001) and in a *daf-16*(*mu86*) loss-of-function mutant (Lin *et al*, 1997). After 12 h of 30°C heat shock, both N2 and *daf-16(mu86)* mutants showed similar levels of ESRE gene upregulation (Figure 2D). Furthermore, a DAF-16-overexpressing strain did not show higher levels of ESRE gene transcription than did N2 controls (data not shown). These data further indicate that DAF-16 does not act through the ESRE network. Nevertheless, we note that there is partial overlap between *daf-16* and *slr-2* stress-related targets. For example, *bona fide daf-16*-dependent genes *sod-3* (Honda and Honda, 1999) and *mtl-1* (Barsyte *et al*, 2001) are not differentially expressed in *slr-2* mutants, whereas *hsp-16.1* and *hsp-16.49*, which are downregulated in *daf-16* mutants (Hsu *et al*, 2003), have an ESRE motif and show three- to four-fold less expression in an *slr-2* background. Despite sharing a number of common targets, our combined data strongly suggest that DAF-16 and SLR-2 function independently to control a largely non-overlapping set of stress target genes.

JMJC-1 is evolutionarily conserved and mediates the ESRE stress response

Although the ESRE motif is conserved across species as evolutionarily diverse as worms, fruit flies, and mammals, *slr-2* does not have any apparent orthologs in non-nematode species. On this basis, we hypothesized that SLR-2 may

control the expression of an evolutionarily conserved regulator of ESRE genes. To test this, we used RNAi to knock down expression of each of the ~40 putative transcriptional regulators that were downregulated in *slr-2* mutants (Kirienko *et al*, 2008) and for which RNAi clones were available (Kamath *et al*, 2003). RNAi-fed worms were then tested for attenuated upregulation of the GFP stress reporters described above. Only one gene, T28F2.4, displayed effects that were similar to *slr-2* (Supplementary Figure S7). T28F2.4 is an uncharacterized gene that encodes a protein containing a putative Jumonji C (JmjC) domain, suggesting that it may have a function in chromatin regulation (Clissold and Ponting, 2001; Ayoub *et al*, 2003). Furthermore, putative T28F2.4 orthologs were identified in fruit flies (CG2982), mice (NO66), and humans (NO66), based on reciprocal best-hit blast *P*-values (Supplementary Figure S8). We heretofore refer to T28F2.4 as *jmjc-1*.

To further characterize the role of *jmjc-1* in stress response, we obtained a deletion allele, *tm3525*, which removes 429 bp including a portion of the third exon. This results in a frameshift and truncation of the C-terminal 628 amino acids from the 748-amino-acid long isoform (T28F2.4a); the 125-amino-acid short isoform (T28F2.4b) is unaffected by the deletion. Similar to *slr-2* mutants, and consistent with RNAi experiments, the 3X-ESRE array showed ~two-fold decrease in fluorescence in *jmjc-1* mutants after stress (Figure 3F). In addition, the majority of ESRE genes in the *jmjc-1(tm3525)* background displayed attenuation of upregulation after heat shock (Figure 2C). Moreover, *jmjc-1* mutants exhibited diminished survival after heat shock and oxidative stress (Figure 5A and B) and reduced short-term recovery after a brief exposure to acute ethanol and hyperosmotic stress (Figure 5C).

We further examined the regulatory relationship between SLR-2 and JMJC-1 using qRT–PCR after stress induction. Consistent with microarray results, expression of *jmjc-1* was reduced in *slr-2* mutants (Figure 6A). In contrast, *slr-2* levels showed no dependence on *jmjc-1* (Figure 6A), suggesting that JMJC-1 acts to regulate the expression of ESRE genes downstream of SLR-2.

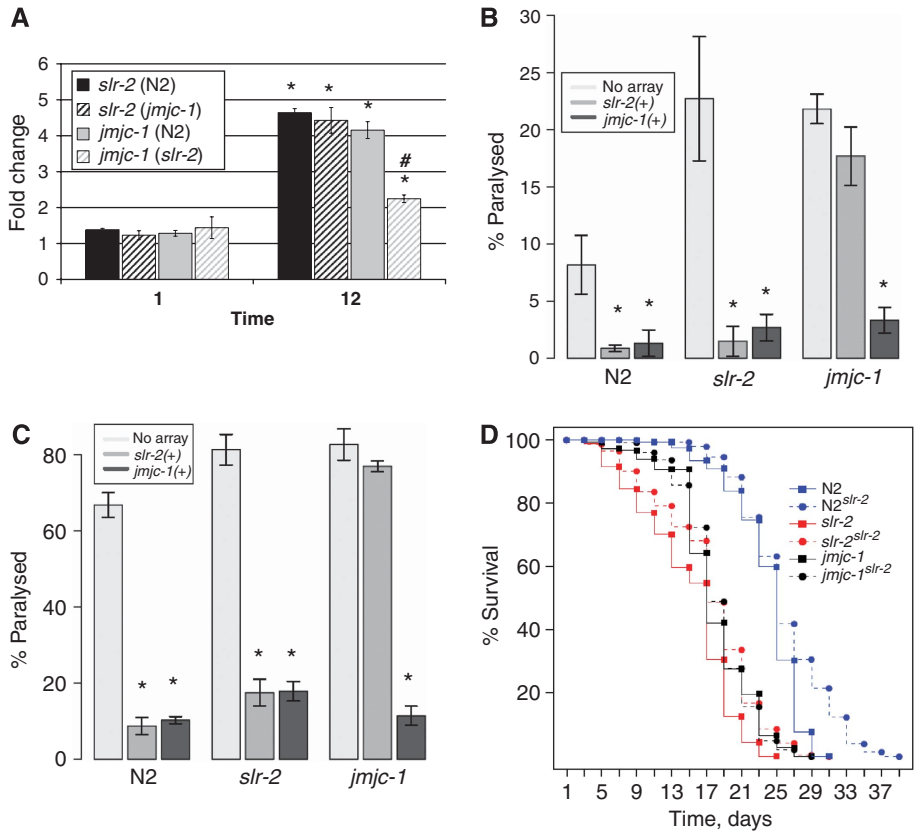

Figure 6 SLR-2–JMJC-1 overexpression and epistasis analysis. (**A**) qRT–PCR data for *slr-2* and *jmjc-1* from heat-shocked *slr-2*(*ku297*), *jmjc-1*(*tm3525*), and wild-type (N2) strains. Note that full induction of *jmjc-1* requires wild-type *slr-2*, whereas *slr-2* expression was not dependent on *jmjc-1*. Asterisks in (**A**) indicate $P<0.01$ as compared with non-stressed genotypic cohorts; hash sign in (**A**) indicates attenuation of upregulation of *jmjc-1* in stressed *slr-2* mutants as compared with stressed wild type ($P<0.01$). (**B**–**C**) Wild-type (N2), *slr-2*(*ku297*), and *jmjc-1*(*tm3525*) worms carrying either no extra-chromosomal array or arrays containing multiple copies of either *slr-2* or *jmjc-1* were subjected to a 12 h ethanol (induced by 4% ethanol-supplemented NGM) (**B**) or oxidative (induced by 160 mM juglone-supplemented NGM) (**C**) stress and scored for paralysis. Asterisks in (**B**) and (**C**) indicate statistical significance, $P< 0.001$. Each bar in (**B**) and (**C**) represents data for 150 animals. Although all three strains showed significant rescue with the extra-chromosomal array encoding *jmjc-1*, the *slr-2* extra-chromosomal array only showed rescue or enhanced survival in *slr-2* and wild-type (N2) strains, further indicating that SLR-2 functions upstream of JMJC-1. (**D**) Survival curves of wild type (N2), *slr-2*(*ku297*), and *jmjc-1*(*tm3525*) with and without the *slr-2* high-copy extra-chromosomal array. Worms were placed at 20°C on NGM plates and scored every other day for survival. In N2 and *slr-2* strains, the *slr-2* extra-chromosomal array conferred a modest, but statistically significant, increase in lifespan ($P<0.001$).

Extra copies of slr-2 and jmjc-1 enhance survival

Given that the loss of *slr-2* and *jmjc-1* results in reduced survival under a variety of stress conditions, we wished to determine whether overexpression of *slr-2* or *jmjc-1* would result in increased longevity or survival under normal or stressed conditions. To do so, we introduced extra-chromosomal arrays containing multiple copies of either *slr-2* (see Kirienko *et al*, 2008 for details) or *jmjc-1* into wild type, *slr-2*, and *jmjc-1* mutants.

Extra copies of either *slr-2* or *jmjc-1* increased survival of wild-type worms on NGM plates supplemented with 4% ethanol (Figure 6B). Similar trends were obtained for oxidative stress, heat shock, and recovery from acute ethanol and salt stresses (Figure 6C; Supplementary Figure S9A–C), suggesting that increased levels of SLR-2 and JMJC-1 are beneficial to survival under conditions of stress. In addition, extra copies of *jmjc-1* increased survival in both *jmjc-1* and *slr-2* mutants whereas overexpression of *slr-2* was beneficial to *slr-2* mutants only. These latter findings are further consistent with JMJC-1 functioning downstream of SLR-2. We next examined whether the presence of a multi-copy *slr-2* extra-chromosomal array could influence longevity by examining the lifespan of wild type, *slr-2*, and *jmjc-1* mutants with and without the array at 16 and 20°C. We observed a modest but statistically significant increase in the mean lifespan of wild-type worms carrying the *slr-2* array at both 20°C (25.7 ± 2.6 versus 27.6 ± 1.7 days) and 16°C (Figure 6D; Supplementary Figure S9D). We note that lifespan extension by *slr-2* overexpression was most evident in the latter third of the time course. The *slr-2* array also augmented lifespan in *slr-2* mutants, although not to wild-type levels, and had no effect on the longevity of *jmjc-1* mutants (Figure 6D; Supplementary Figure S9D). These results suggest that, similar to a number of other stress-response regulatory genes in *C. elegans*, *slr-2* may be capable of promoting longevity.

A Drosophila ortholog of jmjc-1 regulates ESRE genes and is required for survival after stress

To determine whether JMJC-1 has an evolutionarily conserved function in the stress response, we obtained a *D. melanogaster* line with a P-element insertion in CG2982, the fruit fly ortholog of *jmjc-1* (Supplementary Figure S8). In addition to disrupting the coding sequence, the insertion leads to a >2000-fold reduction in transcript levels of CGC2982 (data not shown). We next determined survival rates of young adult female wild type (w^{1118}) and CG2982 mutant (w^{1118}P (EP) $CG2982^{EP1316}$) flies after a 38°C heat shock for 16 h. Consistent with results for *jmjc-1* mutants in *C. elegans*, we observed a dramatic increase in the mortality of CG2982 mutants in multiple biological repeats (Figure 7A). We also assayed expression of CG2982 after a 4 h heat shock and observed an ~three-fold increase in mRNA levels

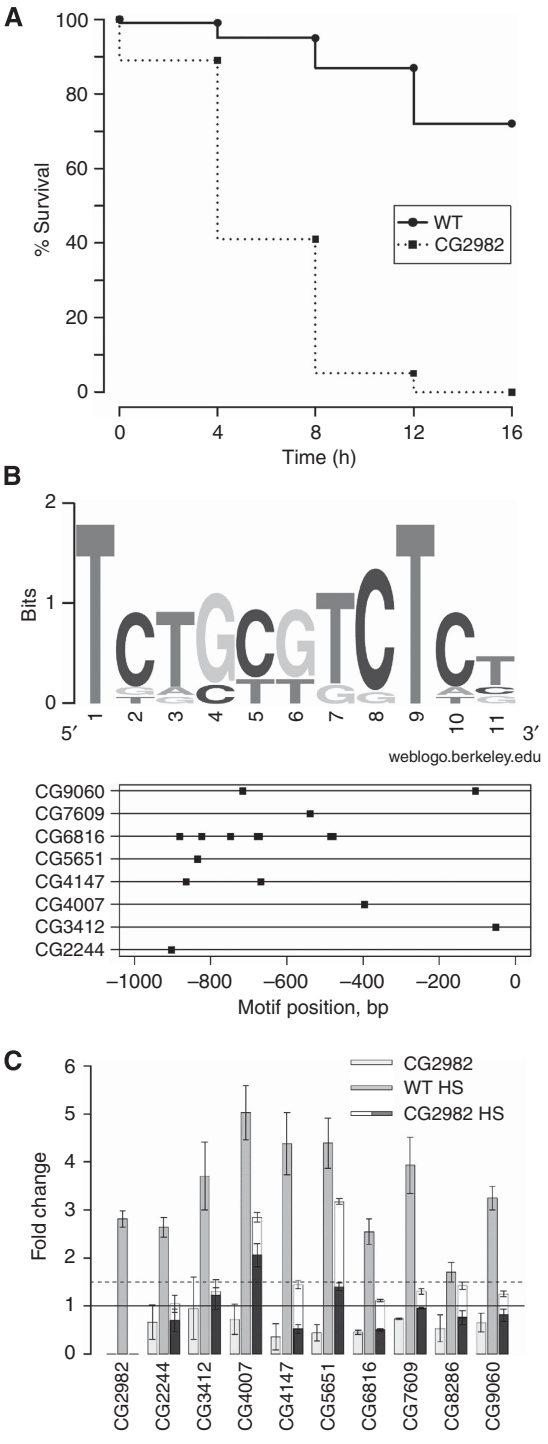

Figure 7 ESRE network conservation in *Drosophila*. (**A**) When exposed to a 16 h lethal heat shock at 38°C, CG2982 mutant flies (w^{1118}P (EP) $CG2982^{EP1316}$) showed dramatically reduced survival as compared with wild-type (w^{1118}) controls (average of three biological replicates, $P<0.001$; $n=115$). (**B**) Logogram and locations of the ESRE motif in *Drosophila* genes tested in (**C**). (**C**) qRT–PCR data are shown from w^{1118}P (EP) $CG2982^{EP1316}$ and w^{1118} control populations subjected to a 4 h, non-lethal 35°C heat shock. Note that CG2982 was upregulated after heat shock in the control strain, but its expression was nearly abolished in the strain carrying the P-element insertion. Furthermore, expression of ESRE genes was attenuated in CG2982 mutants. Light grey bars represent expression of genes in CG2982 mutants normalized to unstressed wild-type controls; grey bars, expression of genes in heat-shocked wild-type flies normalized to unstressed wild-type controls; mixed bars, gene expression in heat-shocked, CG2982 mutants normalized to either unstressed, wild-type controls (dark portion) or unstressed mutants (light portion). In (**C**), solid and dashed lines represent 1- and 1.5-fold change, respectively, and error bars represent s.e.m. Additional statistical information for (**C**) is available in Supplementary Table S1F.

in wild-type flies, consistent with findings in *C. elegans* (Figure 7C). Thus, CG2982 is upregulated after heat shock and is required in flies for survival under heat shock conditions.

We next identified a panel of *Drosophila* ESRE genes based on our derived PWM, which includes several orthologs from our panel of *C. elegans* ESRE genes. The consensus site for our panel and the position of the ESRE motifs within the promoter regions is shown in Figure 7B. Expression of the *Drosophila* gene panel was then monitored by qRT–PCR after heat shock. In all cases, the *Drosophila* ESRE genes showed upregulation of 2.5- to 5-fold (Figure 7C). In contrast, the *Drosophila* ortholog of *dnj-7* (CG8286), which does not contain a recognizable ESRE motif, did not show significant upregulation after heat shock. Notably, the basal level of ESRE gene expression in CG2982 mutants was initially lower than wild type and their upregulation was strongly attenuated (Figure 7C), as was the case in *C. elegans*. Thus, our combined data indicate that both the ESRE network and its regulator JMJC-1 are conserved in worms and flies.

The mammalian ortholog of JMJC-1, NO66, is stress responsive and regulates ESRE gene expression

As we were able to identify a likely ortholog of JMJC-1 in mammals, NO66 (Supplementary Figure S8), we were interested in determining whether the mammalian gene is upregulated in response to stress. To do so, we obtained four mammalian cell culture lines: IEC-6 (rat primary intestinal epithelial cells), NIH-3T3 (immortalized mouse fibroblasts), LAD-II (human primary fibroblasts), and C4-2 (human prostate cancer) cells. Cells were grown to near confluence, and media was replaced with control media or media supplemented with either 70 mM sodium chloride or 200 mM ethanol. RNA was collected after 12 h of treatment and used for cDNA synthesis before qRT–PCR. As observed for *jmjc-1* in *C. elegans* and CG2982 in *D. melanogaster*, mRNA levels of *NO66* were upregulated in all four cell lines after stress (Figure 8A). Sodium chloride increased *NO66* mRNA levels from three- to eight-fold in IEC-6, 3T3, C4-2, and LAD-II cells, whereas ethanol increased mRNA levels by a factor of three- to six-fold in these same lines.

Next, we examined expression levels of eight mammalian ESRE genes (which have orthologs in *C. elegans* that also contain the ESRE motif), in LAD-II cells using qRT–PCR. We observed upregulation of all genes from ~1.5 to 20-fold after 12 h osmotic and ethanol stresses (Figure 8B). As LAD-II primary cells proved recalcitrant to high-efficiency transfection, we used C4-2 cells, which are amenable to transfection (Heemers *et al*, 2007), to test the effect of *NO66* knockdown by siRNA. Targeting of *NO66* by siRNA resulted in an ~4.5-fold reduction in the levels of the *NO66* transcript (based on qRT–PCR; data not shown). Similar to what we observed for ESRE genes in *C. elegans* and *Drosophila*, basal levels of mammalian ESRE genes were reduced ~2–3.5 fold under non-stress conditions (Figure 8C). After ethanol stress, ESRE genes in control siRNA-treated C4-2 cells were increased, although this effect was more modest than in LAD-II primary cells (Figure 8C). Importantly, targeting of *NO66* by siRNA in C4-2 cells strongly attenuated ESRE gene upregulation in response to ethanol stress (Figure 8C). These findings indicate that mammalian NO66 functions analogously to its orthologs in worms and flies to mediate upregulation of ESRE genes in response to stress.

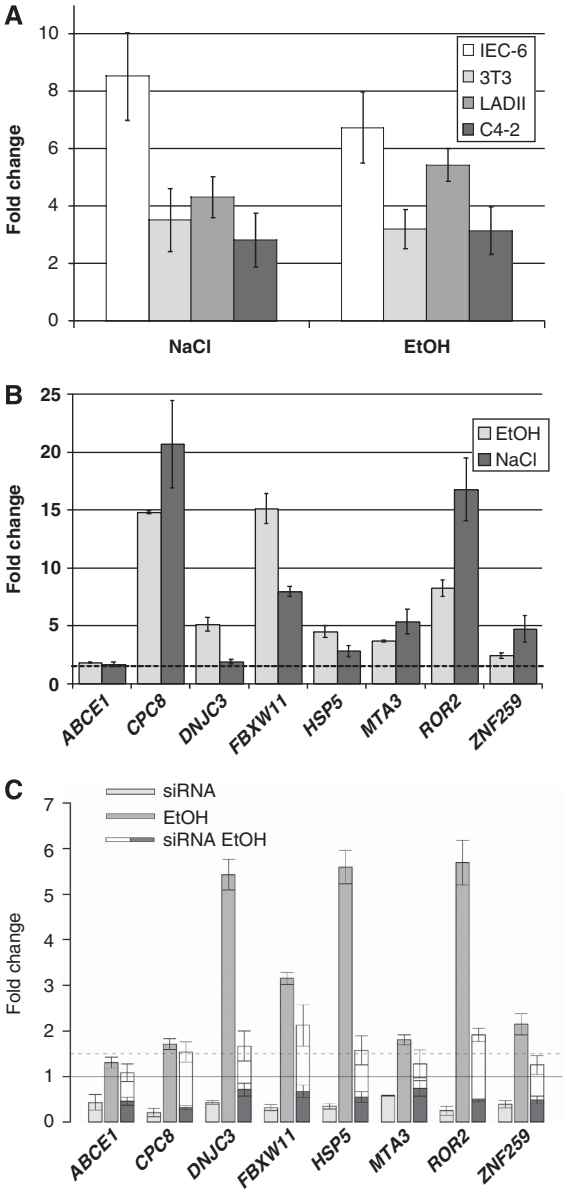

Figure 8 ESRE network conservation in mammals. (**A**) qRT–PCR data for *NO66* expression are shown from IEC-6, 3T3, LAD-II, and C4-2 cell lines subjected to a 12 h treatment with 70 mM NaCl or 200 mM ethanol. (**B**) qRT–PCR data for expression of ESRE-containing mammalian orthologs of *C. elegans* ESRE genes using 70 mM NaCl or 200 mM ethanol-stressed LAD-II cells. (**C**) qRT–PCR data are shown from C4-2 cells transfected with an siRNA construct targeting *NO66* or a control siRNA for 48 h followed by an additional 12 h treatment with 200 mM ethanol. Light grey bars represent expression of genes in unstressed, *NO66* siRNA-treated cells normalized to unstressed cells transfected with a control siRNA; grey bars, expression of genes in ethanol-stressed cells transfected with control siRNA normalized to non-stressed control siRNA; mixed bars, gene expression in ethanol-stressed *NO66* siRNA-treated cells normalized to either ethanol-stressed cells transfected with a control siRNA (dark portion) or to non-stressed *NO66* siRNA-treated cells (light portion). In (**B**) and (**C**), dashed lines represent 1.5-fold. In (**C**), solid line represents 1.0-fold. Error bars in (**A**—**C**) represent s.e.m. In (**A**) and (**B**), all genes assayed showed significant upregulation ($P<0.05$) after ethanol and salt stress as compared with levels in non-stressed controls. Additional statistical information for (**C**) is available in Supplementary Table S1G.

Discussion

In this study, we identified roles for *C. elegans* SLR-2 and JMJC-1 in the response to multiple stress stimuli, including heat shock and osmotic, oxidative, and ethanol stress. The diversity of stress stimuli acting through SLR-2 and JMJC-1 suggests that, similar to DAF-16, these proteins are components of a master stress response network in *C. elegans*. Our data also strongly indicate that JMJC-1, a phylogenetically conserved protein, functions downstream of SLR-2 in this pathway. Bioinformatics, transcriptome, and expression analyses indicate that SLR-2 and JMJC-1 mediate their response to stress through the ESRE regulatory element, a nucleotide motif that is conserved across species. Notably, regulation of stress genes by SLR-2 and JMJC-1 seems to occur independently of the DAF-16 network.

Our report is the first comprehensive analysis on the role of the ESRE motif in pleiotropic stress response. Interestingly, very similar elements were identified earlier in searches for pharyngeal and neuronal tissue-specific enhancers (Gaudet *et al*, 2004; Ruvinsky *et al*, 2007), suggesting that ESRE may also have a function in development. These findings are consistent with a gene mountain distribution analysis (Kim *et al*, 2001) of ESRE SLR-2 targets, which are enriched in heat shock (mountain 20) and neuro-muscular (mountain 1) genes (Supplementary Figure S10). On the basis of our findings, we hypothesize that ESRE acts as a general stress-responsive enhancer element, but that it does not confer tissue specificity. Rather, ESRE may cooperate with additional *cis*-regulatory motifs for determination of cell type-specific expression patterns. This idea is consistent with our observation that stress-induced expression patterns of 3X-ESRE::GFP differed between arrays containing distinct sets of *cis*-regulatory elements (Figure 3; Supplementary Figure S5).

Functional analysis of the JMJC-1 ortholog in *Drosophila* (CG2982) and mammals (NO66) further demonstrated that this gene has an evolutionarily conserved role in the response to stress. In *Drosophila*, CG2982 mRNA is upregulated after heat shock in a similar manner to that observed for *jmjc-1* in *C. elegans*. Analysis of a CG2982 mutant strain further indicated that this gene is required for viability and the robust expression of ESRE genes after heat shock. We also showed that *NO66* mRNAs from mouse, rat, and human cell lines were consistently upregulated in response to multiple stresses. Furthermore, upregulation of mammalian ESRE genes was dependent on *NO66* in human C4-2 cells. Thus, the conservation of the ESRE-regulatory network across these distantly related taxa strongly supports the importance of this previously unrecognized master stress pathway.

NO66 has been reported earlier to have two separate roles (Eilbracht *et al*, 2004; Suzuki *et al*, 2007). The first study suggested that NO66 was localized to the nucleolus in which it colocalizes with regions of late-replicating heterochromatin. NO66 was suggested to promote the maturation and processing of the 90S preribosomal complex, a function that seems to be shared, at least in part, by a paralog, NO52/MINA53 (Eilbracht *et al*, 2004, 2005). NO66 was later reported to activate the expression of target genes, particularly in the presence of a *myc* cofactor, by binding to putative promoter regions and increasing triacylation of histone H4 through the recruitment of a *myc*-regulated histone acetyl transferase complex (Suzuki *et al*, 2007). This latter result is consistent with our findings that JMJC-1/NO66 functions as a transcriptional activator of stress-response genes.

Our studies also add to a growing body of literature closely linking the development and functional maintenance of the gastrointestinal tract of *C. elegans* to the stress response. For example, we have shown earlier that SLR-2 expression is prominent in the intestine and that SLR-2 regulates the expression of many genes required for intestinal functions (Kirienko *et al*, 2008). In addition, PHA-4 (Mango *et al*, 1994) and SKN-1 (Bowerman *et al*, 1992) have established roles in intestinal and foregut development as well as in the oxidative-stress response. Although the connection between these diverse activities remains unclear, the multifunctional nature of many stress-response genes will likely further complicate the task of assigning functions to *C. elegans* stress-response factors.

A significant body of data have intimated a close connection between the molecular mechanisms regulating stress resistance and longevity (Lithgow *et al*, 1995; Johnson *et al*, 1996, 2001; Murphy *et al*, 2003; Oh *et al*, 2005; Chen *et al*, 2007; Samuelson *et al*, 2007; Oliveira *et al*, 2009). Moreover, according to the stress response hypothesis proposed by Johnson et al, much of the increased longevity observed in gerontogene mutants (e.g. *age-1*, *daf-2*, etc.) is due to their greater resistance to exogenous and endogenous stresses (Johnson *et al*, 2001). This hypothesis is supported by findings that overexpression of several stress-response factors, including SKN-1, PHA-4, ABU-11, and DAF-16 increases lifespan (Henderson and Johnson, 2001; Lin *et al*, 2001; Viswanathan *et al*, 2005; Panowski *et al*, 2007; Haskins *et al*, 2008; Tullet *et al*, 2008). Consistent with these findings, we observed a modest, though statistically significant, lifespan extension in strains that carried multiple copies of *slr-2*.

The responses of metazoan organisms to external stress are diverse and complex. It is not surprising, therefore, that these networks have yet to be completely elucidated. It seems probable that a number of master stress regulators, such as SKN-1 and DAF-16, coordinate the input of multiple sensing mechanisms to regulate the expression of large numbers of target genes (An and Blackwell, 2003; McElwee *et al*, 2003, 2004; Murphy *et al*, 2003; Oh *et al*, 2006; Kell *et al*, 2007). Our analysis of SLR-2 and JMJC-1 indicates that these proteins comprise the core of a stress-response pathway that is functionally far reaching and, in the case of JMJC-1 and the ESRE motif, phylogenetically conserved. Further elucidation of the SLR-2–JMJC-1 network in *C. elegans* may therefore provide important insights into stress regulation mechanisms across species.

Materials and methods

C. elegans strains used

C. elegans strains were maintained according to established procedures (Stiernagle, 2006), and all non-heat shock experiments were carried out at 20°C. Strains used in these studies include the following: N2, wild type; CF1038 [*daf-16(mu86)*] (Lin *et al*, 1997); CL924 [*zcIs1, aip*-1::GFP]; CL991 [*kbIs5, gpdh*-1::GFP + pRF4]; CL2070 [*dvIs70, hsp-16*::GFP, (pCL25) + pRF4] (Link *et al*, 1999); CL2166 [*dvIs19, gst-4*::GFP] (Link and Johnson, 2002; Leiers *et al*, 2003); SM1119 [*pSEM599; rol-6*], TJ356 [*daf-16*::GFP*; rol-6*] (Henderson and Johnson, 2001); WY33 [*slr-2(ku297)*] (Kirienko *et al*, 2008); WY286 [*slr-2(ku297); fdEx25*] (Kirienko *et al*, 2008); WY544 [*slr-2*::GFP]; WY547 [*aip-1*::GFP; *slr-2*]; WY548 [*hsp-16*::GFP; *slr-2*]; WY588 [*jmjc-1(tm3525)*], 2× outcrossed; WY589 [*gst-4*::GFP;

slr-2]; and WY592 [*gpdh-1*::GFP; *slr-2*] WY604 [*fdEx25*];. WY611 [*jmjc-1(tm3525); fdEx25*]; WY611 [*jmjc-1(tm3525); fdEx25*]; WY624 [*fdEx82*(*jmjc-1* + *sur-5*::GFP)]; WY627 [*slr-2(ku297)*; *fdEx82* (*jmjc-1* + *sur-5*::GFP)]; WY630 [*jmjc-1(ok3525)*; *fdEx82* (*jmjc-1* + *sur-5*::GFP)]; WY650 [*fdEx88* (*pPD95.77* + *rol-6*)]; WY651 [*fdEx87* (*3X-ExESRE*::GFP + *rol-6*)]; WY665 [*fdEx89* (*3X-ExESRE*::GFP + *sur-5*::GFP)]; WY666 [*fdEx90* (*pPD95.77* + *sur-5*::GFP)].

D. melanogaster strains used
w^{1118} P(EP)CG2982^{EP1316} (Stock Number 11232) and w^{1118} (Stock Number 3605) strains were obtained from the Bloomington Stock Center.

Cell lines used
NIH-3T3, C4-2, IEC-6, and LAD-II cells were grown at 37°C in a humidified 95% O_2/5% CO_2 incubator in Dulbecco's modified essential medium (DMEM, Invitrogen) supplemented with 10% FBS (Invitrogen), and penicillin/streptomycin mix (Invitrogen). Cells were split when they reached 95% confluency.

Nematode stress media
For stress conditions, supplemented NGM medium was used to pour fresh plates the day of the experiment. Plates were spotted with 100 µl of OP50 strain *Escherichia coli* and allowed to dry for approximately 1 h. Plates not used immediately, as well as plates used for longer than 30 min, were sealed with parafilm to minimize drying and evaporation.

Cell culture stress media
DMEM was supplemented with 10% FBS, penicillin/streptomycin, and an appropriate chemical stressor. For experiments using ethanol, the final concentration was 200 mM (Mikami *et al*, 1997; Mashimo *et al*, 1999). For osmotic stress experiments, sodium chloride was added to a final concentration of 70 mM (Perez-Pinera *et al*, 2006). For all experiments, cells were treated for 12 h before collection.

Construction of 3X-ESRE::GFP plasmid
A 3X-ESRE::GFP construct, analogous to previously described (Gaudet *et al*, 2004; Wenick and Hobert, 2004), was generated by PCR amplifying an ~1 kb fragment of pPD95.77, from the *Hind*III to *Eco*RI sites, using the following primers. ESRE_Fwd, 5′-aaaagcttTC TGCGTCTCTTCTGCGTCTCTTCTGCGTCTCTatgcctgcaggtcgactct-3′, pPD_Rev, 5′-CGCTCAGTTGGAATTCTACG-3′. Subsequently, the PCR amplimer was digested with *Hin*dIII and *Eco*RI and cloned into the *Hin*dIII and *Eco*RI sites of pPD95.77. The resulting construct has three, tandem ESRE elements upstream of GFP. Recombinant plasmids were verified by sequencing.

RNAi procedures
RNAi was carried out using standard techniques (Ahringer, 2005). L4 hermaphrodites with stress reporters were placed on RNAi feeding plates. After 4–5 days, F1 progeny at the L4 stage were transferred, either to NGM plates supplemented with 120 µM juglone (Strayer *et al*, 2003), 200 mM NaCl (Hong *et al*, 2004) or to unsupplemented NGM plates. Worms subjected to 30°C heat shock were grown on unsupplemented NGM plates; unsupplemented NGM plates at 20°C were also used as controls for all stress conditions.

siRNA transfection
C4-2 cells were split 1:3 after reaching 90% confluency into media without antibiotics. The next day cells were transfected with 100 pmol C14orf169 Stealth RNAi^{TM} siRNA or 100 pmol of Stealth RNAi siRNA Negative Control Med GC Duplex (Invitrogen) using Lipofectamine2000 reagent (Invitrogen) according to the manufacturer's instructions. In experiments assessing the effects of ethanol stress, medium was replaced with ethanol-supplemented media 24 h post transfection.

Cluster, motif identification, and network analysis
Clustering and regulatory motif analyses were performed essentially as described earlier (Kirienko and Fay, 2007). Cluster visualization was performed using the statistical programming language R (http://www.r-project.org). Network analysis was performed as described earlier (Lee *et al*, 2008). Network visualization was performed using Cytoscape 4.0.

Quantitative real-time reverse transcription–PCR
RNA was extracted from staged L1 larvae, purified, and used for qRT–PCR as described earlier (Kirienko and Fay, 2007) for verification of microarray data. RNA was extracted, purified, and used for qRT–PCR from mixed populations for all other qRT–PCR data. cDNA was prepared from 5 µg total RNA using a SuperScriptII first-strand synthesis system (Invitrogen) following the manufacturer's instructions. qRT–PCR was performed using SYBR Green PCR mastermix (Bio-Rad). qRT–PCR data represent the mean of thre independent biological replicates, each performed in triplicate. Standard error of mean (s.e.m.) represents errors among biological replicates, which we define as independently grown and collected populations of worms, flies, or cells.

Transcriptional fusion reporter quantification
For all transcriptional fusion reporters, staged mid- to late-L4 larvae were used. Images were collected and analysed with OpenLab software. Mean fluorescence was determined for entire organisms and the background fluorescence value was subtracted from each image.

Heat shock
All *C. elegans* heat shock experiments were carried out under one of two conditions: lethal heat shock was performed at 37°C (for survival curves) and non-lethal heat shock at 30°C (for all other experiments) (Fujiwara *et al*, 1999). Heat shock experiments for assaying the level of *hsp-16::GFP* upregulation in mutant and wild-type backgrounds were performed using a 4 h exposure to 30°C. *D. melanogaster* heat shock survival curves were performed at 38°C (Gilchrist *et al*, 1997). For experiments to determine differential regulation of ESRE genes, flies were subjected to a 4 h heat shock at 35°C (Marin *et al*, 1996).

Oxidative stress
Oxidative-stress conditions were carried out using 100 or 120 µM (for transcriptional fusion reporter assays) or 160 µM (for survival curves) *5*-hydroxy-*1,4*-naphthoquinone (juglone) (Strayer *et al*, 2003). For transcriptional fusion reporter assays, mid- to late-L4 larvae were placed on plates, sealed with parafilm, and fluorescence was quantified as described after 4 h (for both *slr-2*::GFP and *gst-4*::GFP) or 12 h (*slr-2*::GFP only). For survival curves, late-L4 larvae were placed on plates containing 160 µM juglone and sealed with parafilm. At appropriate times after being placed on the plate, worms were scored on the basis of a failure to respond to mechanical stimuli.

Ethanol and hypertonic stress recovery
Young adult worms were placed on NGM plates supplemented with 7% (v/w) ethanol (Kwon *et al*, 2004) or 300 mM NaCl. After 30 min, worms were transferred back to NGM plates and allowed to recover for 30 min before being scored. Worms were scored as paralysed if they failed to respond to mechanical stimuli.

Longevity studies
Longevity assays were performed as described earlier (Wolkow *et al*, 2000; Miyata *et al*, 2008). Late-stage L4 hermaphrodites raised at 16° were transferred to NGM plates containing 0.1 mg/ml FUDR, seeded with *E. coli* OP50, and incubated at either 16 or 20°C ($n = 150$ for each temperature and genotype). Lifespan was defined as the length of time from when animals were placed on plates until they were scored as dead on failure to respond to mechanical stimuli.

Statistical analysis
P-values were calculated using *t*-tests and χ^2 tests with the statistical programming language R. Log-rank tests for longevity curves were performed using software available at http://bioinf.wehi.edu.au/software/russell/logrank/.

Supplementary data
Supplementary data are available at *The EMBO Journal* Online (http://www.embojournal.org).

Acknowledgements

We thank Chris Link, Tom Johnson, Jeb Gaudet, the *Caenorhabditis* Genetics Center, and the National Bioresource Project for the Experimental Animal *C. elegans* (Japan) for generously providing strains. We also thank the Bloomington *Drosophila* Stock Center for *D. melanogaster* strains. C4-2 and IEC-6 cells were generously provided by Ji Li at the University of Wyoming, 3T3 cells were kindly provided by Patrick Johnson at the University of Wyoming. LAD-II cells were a generous gift from Martin Wild and Dietmar Vestweber at the Max Planck Institute of Molecular Biomedicine. We thank Don Jarvis for aid and input with cell culture. We thank Amy Fluet, Chris Link, and Daniel Hill for useful input. This work was supported by NIH grant GM066868 and by INBRE P20RR016474.

Conflict of interest

The authors declare that they have no conflict of interest.

References

Ahringer J (2005) *Reverse Genetics*. WormBook (The C. elegans Research Community, ed.) http://www.wormbook.org/

An JH, Blackwell TK (2003) SKN-1 links C. elegans mesendodermal specification to a conserved oxidative stress response. *Genes Dev* **17:** 1882–1893

Ayoub N, Noma K, Isaac S, Kahan T, Grewal SI, Cohen A (2003) A novel jmjC domain protein modulates heterochromatization in fission yeast. *Mol Cell Biol* **23:** 4356–4370

Barsyte D, Lovejoy DA, Lithgow GJ (2001) Longevity and heavy metal resistance in daf-2 and age-1 long-lived mutants of Caenorhabditis elegans. *FASEB J* **15:** 627–634

Baumeister R, Schaffitzel E, Hertweck M (2006) Endocrine signaling in Caenorhabditis elegans controls stress response and longevity. *J Endocrinol* **190:** 191–202

Berdichevsky A, Guarente L (2006) A stress response pathway involving sirtuins, forkheads and 14–3–3 proteins. *Cell Cycle* **5:** 2588–2591

Berdichevsky A, Viswanathan M, Horvitz HR, Guarente L. (2006) C. elegans SIR-2.1 interacts with 14–3–3 proteins to activate DAF-16 and extend life span. *Cell* **125:** 1165–1177

Bowerman B, Eaton BA, Priess JR (1992) skn-1, a maternally expressed gene required to specify the fate of ventral blastomeres in the early C. elegans embryo. *Cell* **68:** 1061–1075

Candido EP, Jones D, Dixon DK, Graham RW, Russnak RH, Kay RJ (1989) Structure, organization, and expression of the 16-kDa heat shock gene family of Caenorhabditis elegans. *Genome* **31:** 690–697

Chen D, Pan KZ, Palter JE, Kapahi P (2007) Longevity determined by developmental arrest genes in Caenorhabditis elegans. *Aging Cell* **6:** 525–533

Clissold PM, Ponting CP (2001) JmjC: cupin metalloenzyme-like domains in jumonji, hairless and phospholipase A2beta. *Trends Biochem Sci* **26:** 7–9

Eilbracht J, Kneissel S, Hofmann A, Schmidt-Zachmann MS (2005) Protein NO52–a constitutive nucleolar component sharing high sequence homologies to protein NO66. *Eur J Cell Biol* **84:** 279–294

Eilbracht J, Reichenzeller M, Hergt M, Schnolzer M, Heid H, Stohr M, Franke WW, Schmidt-Zachmann MS (2004) NO66, a highly conserved dual location protein in the nucleolus and in a special type of synchronously replicating chromatin. *Mol Biol Cell* **15:** 1816–1832

Falk MJ, Zhang Z, Rosenjack JR, Nissim I, Daikhin E, Nissim I, Sedensky MM, Yudkoff M, Morgan PG (2008) Metabolic pathway profiling of mitochondrial respiratory chain mutants in C. elegans. *Mol Genet Metab* **93:** 388–397

Fujiwara M, Ishihara T, Katsura I (1999) A novel WD40 protein, CHE-2, acts cell-autonomously in the formation of C. elegans sensory cilia. *Development* **126:** 4839–4848

Furuyama T, Nakazawa T, Nakano I, Mori N (2000) Identification of the differential distribution patterns of mRNAs and consensus binding sequences for mouse DAF-16 homologues. *Biochem J* **349:** 629–634

Garigan D, Hsu AL, Fraser AG, Kamath RS, Ahringer J, Kenyon C (2002) Genetic analysis of tissue aging in Caenorhabditis elegans: a role for heat-shock factor and bacterial proliferation. *Genetics* **161:** 1101–1112

Gaudet J, Muttumu S, Horner M, Mango SE (2004) Whole-genome analysis of temporal gene expression during foregut development. *PLoS Biol* **2:** e352

Gilchrist GW, Huey RB, Partridge L (1997) Thermal sensitivity of Drosophila melanogaster: evolutionary responses of adults and eggs to laboratory natural selection at different temperatures. *Physiol Zool* **70:** 403–414

GuhaThakurta D, Palomar L, Stormo GD, Tedesco P, Johnson TE, Walker DW, Lithgow G, Kim S, Link CD (2002) Identification of a novel cis-regulatory element involved in the heat shock response in Caenorhabditis elegans using microarray gene expression and computational methods. *Genome Res* **12:** 701–712

Hasegawa K, Miwa S, Tajima T, Tsutsumiuchi K, Taniguchi H, Miwa J (2007) A rapid and inexpensive method to screen for common foods that reduce the action of acrylamide, a harmful substance in food. *Toxicol Lett* **175:** 82–88

Haskins KA, Russell JF, Gaddis N, Dressman HK, Aballay A (2008) Unfolded protein response genes regulated by CED-1 are required for Caenorhabditis elegans innate immunity. *Dev Cell* **15:** 87–97

Hassan WM, Merin DA, Fonte V, Link CD (2009) AIP-1 ameliorates beta-amyloid peptide toxicity in a Caenorhabditis elegans Alzheimer's disease model. *Hum Mol Genet* **18:** 2739–2747

Heemers HV, Regan KM, Dehm SM, Tindall DJ (2007) Androgen induction of the androgen receptor coactivator four and a half LIM domain protein-2: evidence for a role for serum response factor in prostate cancer. *Cancer Res* **67:** 10592–10599

Henderson ST, Johnson TE (2001) daf-16 integrates developmental and environmental inputs to mediate aging in the nematode Caenorhabditis elegans. *Curr Biol* **11:** 1975–1980

Hertweck M, Hoppe T, Baumeister R (2003) C. elegans, a model for aging with high-throughput capacity. *Exp Gerontol* **38:** 345–346

Honda Y, Honda S (1999) The daf-2 gene network for longevity regulates oxidative stress resistance and Mn-superoxide dismutase gene expression in Caenorhabditis elegans. *FASEB J* **13:** 1385–1393

Hong M, Kwon JY, Shim J, Lee J (2004) Differential hypoxia response of hsp-16 genes in the nematode. *J Mol Biol* **344:** 369–381

Hsu AL, Murphy CT, Kenyon C (2003) Regulation of aging and age-related disease by DAF-16 and heat-shock factor. *Science* **300:** 1142–1145

Johnson TE, Cypser J, de Castro E, de Castro S, Henderson S, Murakami S, Rikke B, Tedesco P, Link C (2000) Gerontogenes mediate health and longevity in nematodes through increasing resistance to environmental toxins and stressors. *Exp Gerontol* **35:** 687–694

Johnson TE, de Castro E, Hegi de Castro S, Cypser J, Henderson S, Tedesco P (2001) Relationship between increased longevity and stress resistance as assessed through gerontogene mutations in Caenorhabditis elegans. *Exp Gerontol* **36:** 1609–1617

Johnson TE, Henderson S, Murakami S, de Castro E, de Castro SH, Cypser J, Rikke B, Tedesco P, Link C (2002) Longevity genes in the nematode Caenorhabditis elegans also mediate increased resistance to stress and prevent disease. *J Inherit Metab Dis* **25:** 197–206

Johnson TE, Lithgow GJ, Murakami S (1996) Hypothesis: interventions that increase the response to stress offer the potential for effective life prolongation and increased health. *J Gerontol A Biol Sci Med Sci* **51:** B392–B395

Kahn NW, Rea SL, Moyle S, Kell A, Johnson TE (2008) Proteasomal dysfunction activates the transcription factor SKN-1 and produces a selective oxidative-stress response in Caenorhabditis elegans. *Biochem J* **409:** 205–213

Kamath RS, Fraser AG, Dong Y, Poulin G, Durbin R, Gotta M, Kanapin A, Le Bot N, Moreno S, Sohrmann M, Welchman DP, Zipperlen P, Ahringer J (2003) Systematic functional analysis of

the Caenorhabditis elegans genome using RNAi. *Nature* **421:** 231–237

Kell A, Ventura N, Kahn N, Johnson TE (2007) Activation of SKN-1 by novel kinases in Caenorhabditis elegans. *Free Radic Biol Med* **43:** 1560–1566

Kim SK, Lund J, Kiraly M, Duke K, Jiang M, Stuart JM, Eizinger A, Wylie BN, Davidson GS (2001) A gene expression map for Caenorhabditis elegans. *Science* **293:** 2087–2092

Kirienko NV, Fay DS (2007) Transcriptome profiling of the C. elegans Rb ortholog reveals diverse developmental roles. *Dev Biol* **305:** 674–684

Kirienko NV, McEnerney JD, Fay DS (2008) Coordinated regulation of intestinal functions in C elegans by LIN- 35/Rb and SLR-. *PLoS Genet* **4:** e1000059

Kwon JY, Hong M, Choi MS, Kang S, Duke K, Kim S, Lee S, Lee J (2004) Ethanol-response genes and their regulation analyzed by a microarray and comparative genomic approach in the nematode Caenorhabditis elegans. *Genomics* **83:** 600–614

Lamitina ST, Strange K (2005) Transcriptional targets of DAF-16 insulin signaling pathway protect C. elegans from extreme hypertonic stress. *Am J Physiol Cell Physiol* **288:** C467–C474

Lamitina T, Huang CG, Strange K (2006) Genome-wide RNAi screening identifies protein damage as a regulator of osmoprotective gene expression. *Proc Natl Acad Sci USA* **103:** 12173–12178

Lee I, Lehner B, Crombie C, Wong W, Fraser AG, Marcotte EM (2008) A single gene network accurately predicts phenotypic effects of gene perturbation in Caenorhabditis elegans. *Nat Genet* **40:** 181–188

Leiers B, Kampkotter A, Grevelding CG, Link CD, Johnson TE, Henkle-Duhrsen K (2003) A stress-responsive glutathione S-transferase confers resistance to oxidative stress in Caenorhabditis elegans. *Free Radic Biol Med* **34:** 1405–1415

Lin K, Dorman JB, Rodan A, Kenyon C (1997) daf-16: an HNF-3/forkhead family member that can function to double the life-span of Caenorhabditis elegans. *Science* **278:** 1319–1322

Lin K, Hsin H, Libina N, Kenyon C (2001) Regulation of the Caenorhabditis elegans longevity protein DAF-16 by insulin/IGF-1 and germline signaling. *Nat Genet* **28:** 139–145

Link CD, Cypser JR, Johnson CJ, Johnson TE (1999) Direct observation of stress response in Caenorhabditis elegans using a reporter transgene. *Cell Stress Chaperones* **4:** 235–242

Link CD, Johnson CJ (2002) Reporter transgenes for study of oxidant stress in Caenorhabditis elegans. *Methods Enzymol* **353:** 497–505

Lithgow GJ, White TM, Melov S, Johnson TE (1995) Thermotolerance and extended life-span conferred by single-gene mutations and induced by thermal stress. *Proc Natl Acad Sci USA* **92:** 7540–7544

Mango SE, Lambie EJ, Kimble J (1994) The pha-4 gene is required to generate the pharyngeal primordium of Caenorhabditis elegans. *Development* **120:** 3019–3031

Marin R, Demers M, Tanguay RM (1996) Cell-specific heat-shock induction of Hsp23 in the eye of Drosophila melanogaster. *Cell Stress Chaperones* **1:** 40–46

Mashimo K, Haseba T, Ohno Y (1999) Flow cytometric and fluorescence microscopic analysis of ethanol-induced G2 + M block: ethanol dose-dependently delays the progression of the M phase. *Alcohol Alcohol* **34:** 300–310

McElwee J, Bubb K, Thomas JH (2003) Transcriptional outputs of the Caenorhabditis elegans forkhead protein DAF-16. *Aging Cell* **2:** 111–121

McElwee JJ, Schuster E, Blanc E, Thomas JH, Gems D (2004) Shared transcriptional signature in Caenorhabditis elegans Dauer larvae and long-lived daf-2 mutants implicates detoxification system in longevity assurance. *J Biol Chem* **279:** 44533–44543

Mikami K, Haseba T, Ohno Y (1997) Ethanol induces transient arrest of cell division (G2 + M block) followed by G0/G1 block: dose effects of short- and longer-term ethanol exposure on cell cycle and cell functions. *Alcohol Alcohol* **32:** 145–152

Miyata S, Begun J, Troemel ER, Ausubel FM (2008) DAF-16-dependent suppression of immunity during reproduction in Caenorhabditis elegans. *Genetics* **178:** 903–918

Mukhopadhyay A, Tissenbaum HA (2007) Reproduction and longevity: secrets revealed by C. elegans. *Trends Cell Biol* **17:** 65–71

Murakami S, Johnson TE (1996) A genetic pathway conferring life extension and resistance to UV stress in Caenorhabditis elegans. *Genetics* **143:** 1207–1218

Murphy CT, McCarroll SA, Bargmann CI, Fraser A, Kamath RS, Ahringer J, Li H, Kenyon C (2003) Genes that act downstream of DAF-16 to influence the lifespan of Caenorhabditis elegans. *Nature* **424:** 277–283

Oh SW, Mukhopadhyay A, Dixit BL, Raha T, Green MR, Tissenbaum HA (2006) Identification of direct DAF-16 targets controlling longevity, metabolism and diapause by chromatin immunoprecipitation. *Nat Genet* **38:** 251–257

Oh SW, Mukhopadhyay A, Svrzikapa N, Jiang F, Davis RJ, Tissenbaum HA (2005) JNK regulates lifespan in Caenorhabditis elegans by modulating nuclear translocation of forkhead transcription factor/DAF-16. *Proc Natl Acad Sci USA* **102:** 4494–4499

Oliveira RP, Abate JP, Dilks K, Landis J, Ashraf J, Murphy CT, Blackwell TK (2009) Condition-adapted stress and longevity gene regulation by Caenorhabditis elegans SKN-1/Nrf. *Aging Cell* **8:** 524–541

Panowski SH, Wolff S, Aguilaniu H, Durieux J, Dillin A (2007) PHA-4/Foxa mediates diet-restriction-induced longevity of C. elegans. *Nature* **447:** 550–555

Perez-Pinera P, Menendez-Gonzalez M, del Valle M, Vega JA (2006) Sodium chloride regulates Extracellular Regulated Kinase 1/2 in different tumor cell lines. *Mol Cell Biochem* **293:** 93–101

Ruvinsky I, Ohler U, Burge CB, Ruvkun G (2007) Detection of broadly expressed neuronal genes in C. elegans. *Dev Biol* **302:** 617–626

Sampayo JN, Olsen A, Lithgow GJ (2003) Oxidative stress in Caenorhabditis elegans: protective effects of superoxide dismutase/catalase mimetics. *Aging Cell* **2:** 319–326

Samuelson AV, Klimczak RR, Thompson DB, Carr CE, Ruvkun G (2007) Identification of Caenorhabditis elegans genes regulating longevity using enhanced RNAi-sensitive strains. *Cold Spring Harb Symp Quant Biol* **72:** 489–497

Singh V, Aballay A (2006) Heat-shock transcription factor (HSF)-1 pathway required for Caenorhabditis elegans immunity. *Proc Natl Acad Sci USA* **103:** 13092–13097

Stiernagle T (2006) *Maintenance of C. elegans WormBook*, (The C. elegans Research Community, ed.) http://www.wormbook.org/

Strayer A, Wu Z, Christen Y, Link CD, Luo Y (2003) Expression of the small heat-shock protein Hsp16-2 in Caenorhabditis elegans is suppressed by Ginkgo biloba extract EGb 761. *FASEB J* **17:** 2305–2307

Suzuki C, Takahashi K, Hayama S, Ishikawa N, Kato T, Ito T, Tsuchiya E, Nakamura Y, Daigo Y (2007) Identification of Myc-associated protein with JmjC domain as a novel therapeutic target oncogene for lung cancer. *Mol Cancer Ther* **6:** 542–551

Troemel ER, Chu SW, Reinke V, Lee SS, Ausubel FM, Kim DH (2006) p38 MAPK regulates expression of immune response genes and contributes to longevity in C. elegans. *PLoS Genet* **2:** e183

Tullet JM, Hertweck M, An JH, Baker J, Hwang JY, Liu S, Oliveira RP, Baumeister R, Blackwell TK (2008) Direct inhibition of the longevity-promoting factor SKN-1 by insulin-like signaling in C. elegans. *Cell* **132:** 1025–1038

Viswanathan M, Kim SK, Berdichevsky A, Guarente L (2005) A role for SIR-2.1 regulation of ER stress response genes in determining C. elegans life span. *Dev Cell* **9:** 605–615

Wenick AS, Hobert O (2004) Genomic cis-regulatory architecture and trans-acting regulators of a single interneuron-specific gene battery in C. elegans. *Dev Cell* **6:** 757–770

Wolkow CA, Kimura KD, Lee MS, Ruvkun G (2000) Regulation of C. elegans life-span by insulinlike signaling in the nervous system. *Science* **290:** 147–150

Wu D, Rea SL, Yashin AI, Johnson TE (2006) Visualizing hidden heterogeneity in isogenic populations of C. elegans. *Exp Gerontol* **41:** 261–270